

# Visualisation Techniques for Random Telegraph Signals in MOSFETs

Arnoud P. van der Wel, Eric A. M. Klumperink, Jay Kolhatkar, Erik Hoekstra and Bram Nauta

email: a.p.vanderwel@utwente.nl

URL: icd.ewi.utwente.nl

**Abstract**—In the study of LF noise in MOSFETs, it has become clear that Random Telegraph Signals (RTS) are dominant. When a MOSFET is subjected to large-signal excitation, the RTS noise is influenced. In this paper, we present different visualizations of the transient behaviour of the RTS.

**Keywords**—MOSFET, Random Telegraph Signal, Large Signal Excitation, LF Noise.

## I. INTRODUCTION

Increasing integration of analog functionality with digital processing power fuels the desire to realize analog circuitry in CMOS. This has led to a multitude of interesting analog challenges and solutions. Complication comes from the supply voltage that drops in each next process generation, making the available signal swing smaller and smaller. At the other end of the magnitude spectrum, LF noise limits the available dynamic range.

MOSFETs are notorious for their LF noise. LF Noise in MOSFETs is often roughly characterized by a  $1/f$  corner frequency  $f_c$ , below which the LF noise PSD of the device rises with approximately  $1/f$ . It can be shown [1] that the  $1/f$  noise corner frequency of MOSFETs scales with the transit frequency  $f_t$  of the device, so that as MOSFETs become faster, they also become noisier. In MOSFETs of modern submicron CMOS processes, the  $f_c$  can be as high as several tens of MHz, which means that anything below that has to be considered 'low frequency' as far as noise performance is concerned. LF noise, however, is not only a problem for LF circuit design, but also for RF applications. For example, in VCO's, LF device noise is upconverted to reappear as close-in phase noise of the oscillator. The phase noise of RF DLL's and PLL's is also critically limited by LF noise of the active devices.

$1/f$  Noise is found in all sorts of physical systems [2]. This has led to a lot of speculation on the physical origins of  $1/f$  noise and the idea that there might be a common physical thermodynamic [3] or quantummechanical [4] origin for all the  $1/f$  noise we observe. In MOSFETs, one of the best characterized  $1/f$  noise sources available today, the search for the origins of the noise has led to two likely candidates: mobility fluctuations ( $\Delta\mu$ -model) and

number fluctuations ( $\Delta N$ -model). In homogenous semiconductor samples,  $1/f$  noise caused by mobility fluctuations ( $\Delta\mu$ ) has been observed [5]. It can be shown that if a MOSFET is 'small enough'; i.e. the number of free carriers is low enough, its LF noise will be dominated by trapping-detrapping (RTS) noise ( $\Delta N$  model) rather than mobility-based  $1/f$  noise ( $\Delta\mu$  model) [6]. Modern submicron MOSFETs clearly fall into this category, and their LF noise is dominated by RTS [7]. The classical derivation that trapping-detrapping can lead to a  $1/f$  spectrum was given by McWorther in 1957 [8], though it was later shown by several authors that the conditions for the emergence of a  $1/f$  spectrum as given by McWorther are more severe than necessary [9].

The study and modelling of LF noise in MOSFETs is commonly done by measurement, where a device is biased at a certain point in its operating range, and the LF noise PSD measured. This is done for several operating points, and careful parameter extraction has led to quite detailed bias-dependent noise models for MOSFETs [10]. However, all such measurements are carried out in steady state. Circuit simulators, on which analog designers depend for optimal circuit design, follow this approach and model the LF noise voltage as a function of the bias voltage. However, even the best circuit simulators [11] still always model the LF noise as an instantaneous function of the bias voltage. This is unfortunately too simplistic an approach.

In real circuits, signal swings are not 'small' in comparison to the bias voltage. Small signal analysis breaks down in these cases, and small signal noise analysis (even with a time-variant operating point as in a PSS or a Pnoise simulation) will not give correct results. The reason for this is that the LF noise of a MOSFET is not only a function of the current bias of the device, but also of the bias history of the device [12], [13]. What this means is that if the frequency of excitation is larger than the frequency of the LF noise, the quasi-static approach to LF noise (as used by simulators) is not valid.

The unsatisfactory situation with respect to simulation possibilities, coupled with the dominant RTS noise in small MOSFETs and the large-signal conditions encoun-

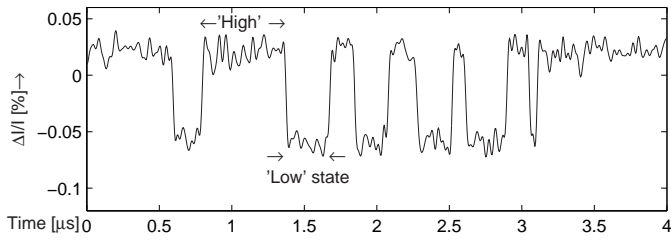


Fig. 1. A Random Telegraph Signal.

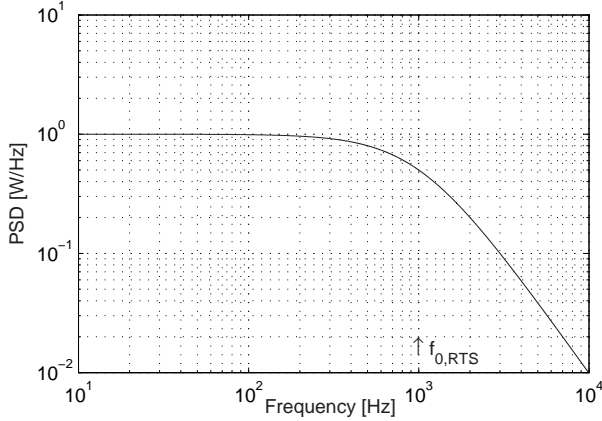


Fig. 2. PSD of a Random Telegraph Signal.

tered in many circuits mean that it is very relevant to research this combination of topics further. This is what we do in this paper.

## II. TIME-DOMAIN ANALYSIS

A Random Telegraph signal is a time-continuous, amplitude-discrete signal that is characterized by three parameters: the mean low time, the mean high time and the amplitude (fig. 1). The autocorrelation function of such a signal was derived by Machlup in 1954 [14]. Using the autocorrelation function the power spectral density of the signal may be calculated. This is a Lorentzian (fig. 2): flat at low frequencies, and decaying with  $-20\text{dB/dec}$  above some corner frequency  $f_{0,RTS}$ . Though the frequency and time domain description are fundamentally equivalent, the time-domain description is more complete, as witnessed by the fact that there are three parameters in the time domain, and only two in the frequency domain.

Though the study of LF noise under transient conditions can be carried out in the frequency domain [15], [16], the fact that we are dealing with RTS noise in this case means that a time-domain analysis is more appropriate since it gives us all the information we want in a raw form, without any post-processing. This also facilitates modelling efforts [17].

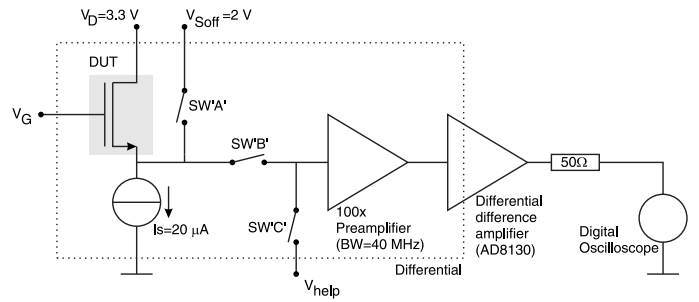


Fig. 3. Measurement Setup.

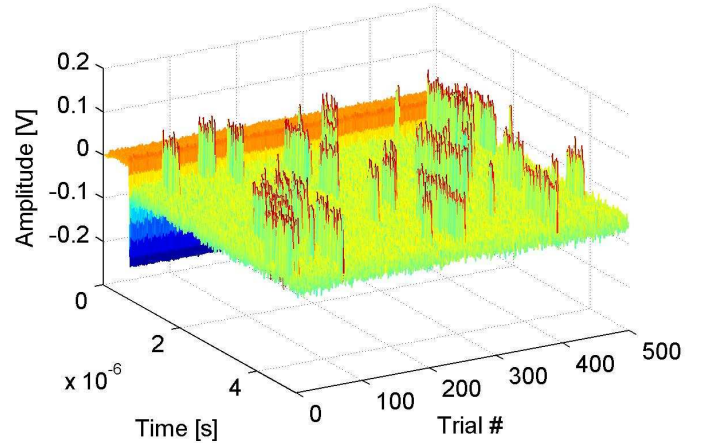


Fig. 4. Time domain view of RTS.

## III. MEASUREMENT METHOD

To study RTS noise under transient conditions in the time domain, we make use of the measurement setup of fig. 3. The device in question can be either subjected to a constant bias or time-variant bias. For the constant bias measurement, the preamps and switches are operated in precisely the same way as for the transient measurement; only the device is constantly kept in a particular bias state. The 'front end' of the measurement setup is completely differential. In this way, a differential preamp can be used to suppress the large common mode signal that accompanies the bias transients applied to the DUTs, and the dynamic range requirement of the oscilloscope is reduced.

Measurements are carried out on several devices with a W/L of between  $0.5/0.35 \mu\text{m}$  and  $1.25/0.575 \mu\text{m}$  from an industrial  $0.35 \mu\text{m}$  process.  $t_{ox}$  is  $7.5 \text{ nm}$ .  $I_d$  is  $20 \mu\text{A}$  per device. The devices are cycled on and off with a frequency of  $100 \text{ Hz}$ ; the duty cycle is  $50\%$ . After a turn-on transient, the first  $5 \mu\text{s}$  of noise are measured. 1 second later, this measurement is repeated. In this way, 500 trials of the experiment are performed.

A sample result is shown in fig. 4. Time, from 0 to  $5 \mu\text{s}$  is along the x-axis, and the trial # is along the y-axis. The measured noise voltage is the z-value of this plot. To

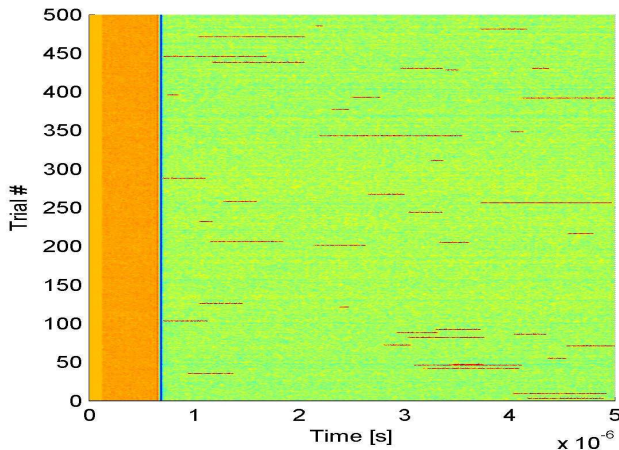


Fig. 5. 'Top view' of RTS.

make sure we don't miss any interesting transient effects, we start each plot briefly ( $0.5\mu\text{s}$ ) before the moment we turn the device on, so that the complete turn-on transient is visible. This is the case for the steady state measurement but also for the transient measurement.

The trial# (y) axis in these plots can be interpreted as a 'slow' time axis; the scale is not exactly known due to limitations in the experimental setup, but is of the order of 500 seconds total. In this way, a clear distinction can be made between 'fast' effects (along the x-axis) and 'slow' effects (along the y-axis). The noise voltage is color-coded, and this raises the possibility of viewing the 3-d plot from above. This is done in fig. 5. The turn-on transient is now visible to the left of the plot, and again, fast effects are visible along the x-axis, and slow effects along the y-axis. Both views are useful in the interpretation of the results.

We can also post-process the time-domain data further. The most obvious thing to do is to examine the average noise voltage at each time instant following the turn-on transient, and the variance of the noise voltage at each time instant. This is illustrated in fig. 6.

In some circuits, e.g. sampling circuits, an obvious approach is to keep the device 'off' until briefly before the device is required to be active. If the variance of the noise at the time that the device is used (eg. to take a sample) is lower than in steady state, then turning the device 'off' when it is not required is a beneficial technique with respect to the noise performance.

#### IV. MEASUREMENT RESULTS

Measurements were carried out on 30 devices. We will discuss some of the most interesting observations below.

The result in fig. 7 shows that a slow RTS (time constant of the order of several tens of seconds) that is present in the steady state case (upper figure) is completely absent just

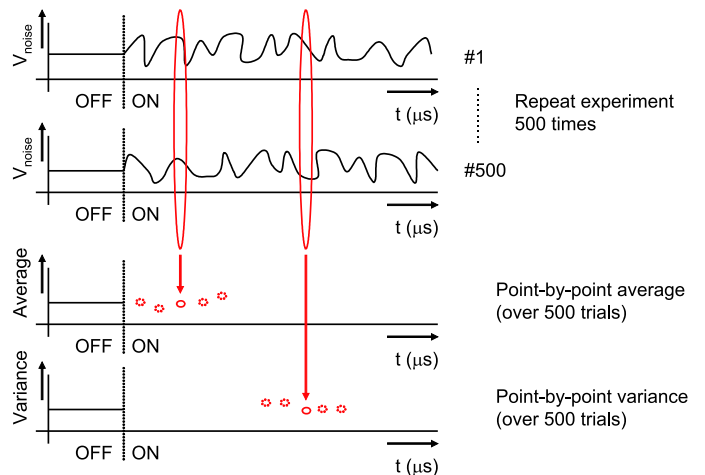


Fig. 6. Calculating average and variance from time-domain data.

after turning the device on (lower figure).

In fig. 8, measurement results for the same device as fig. 4 and 5 are given. In the steady state, (upper figure), the RTS is mostly in the 'low' state with occasional brief excursions into the 'high' state. The RTS decays back to the ground state after a brief time of the order of  $1\mu\text{s}$ . Immediately after turn-on (lower figure), the RTS in this device starts in the 'high' state, after which it can be seen to decay back into the 'low' state after a few  $\mu\text{s}$ .

For the same device, we have plotted the variance and average of the noise immediately after turn-on in fig. 9. The average value of the noise voltage has a slow tail after turn-on, of the order of  $2\mu\text{s}$ . The variance of the noise is also seen to have a maximum just after turn-on; this is the average time before the RTS decays back into its 'low' state.

In fig. 10, yet another kind of interesting behaviour is observed. Whereas in the steady state (upper figure), the RTS is mostly in the 'high' state (red), with occasional brief excursions into the 'low' state (blue), the behaviour of this device immediately after turn-on (lower figure) is exactly the opposite. There obviously has to be some transition between the two, but this is not visible in the figure due to the limited observation time of  $5\mu\text{s}$  for each trial. This is clearly a case where there are two different RTS present in the device, one fast one (visible in both the upper and lower figure) and a slow one responsible for the difference between the upper and lower figure.

#### V. DISCUSSION

Though obviously very useful for insight into the behaviour of RTS noise, there are some limitations that have to be considered. First of all, it is not difficult to de-

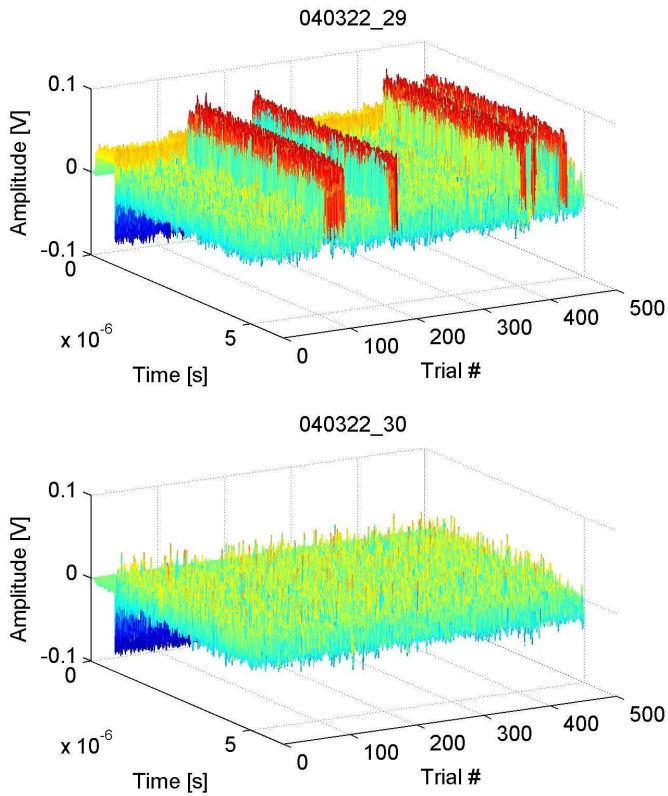


Fig. 7. Large-amplitude, slow RTS (upper figure) is not present immediately after turn-on (lower figure).

duce that when observing an RTS in a single n-channel device, the high-current state corresponds to the unfilled (detrapped) state of the trap, and that the low-current state corresponds to the filled (trapped) state of the trap. This is interesting information in the study of traps, however unfortunately, in the present measurement setup, this information is lost because the measurement setup is differential. We may observe an RTS, but we cannot be sure whether it is in the one or the other device. Single ended measurements do not have this problem but are much more sensitive to noise and crosstalk from the various parts of the setup. Another possibility to overcome this limitation while retaining the benefits of a differential measurement setup is to slightly vary the gate bias around the bias point of interest. By observation in which direction the trap reacts to the varying gate voltage, conclusions about what is the the trapped and the detrapped state of the trap may be drawn. [18]

Secondly, we have presented a somewhat rosy picture of reality by presenting only the most interesting behaviour of the 30 devices measured. In fact, many devices show no significant LF noise change in reaction to transient conditions at all. Moreover, as we are unable to qualify what

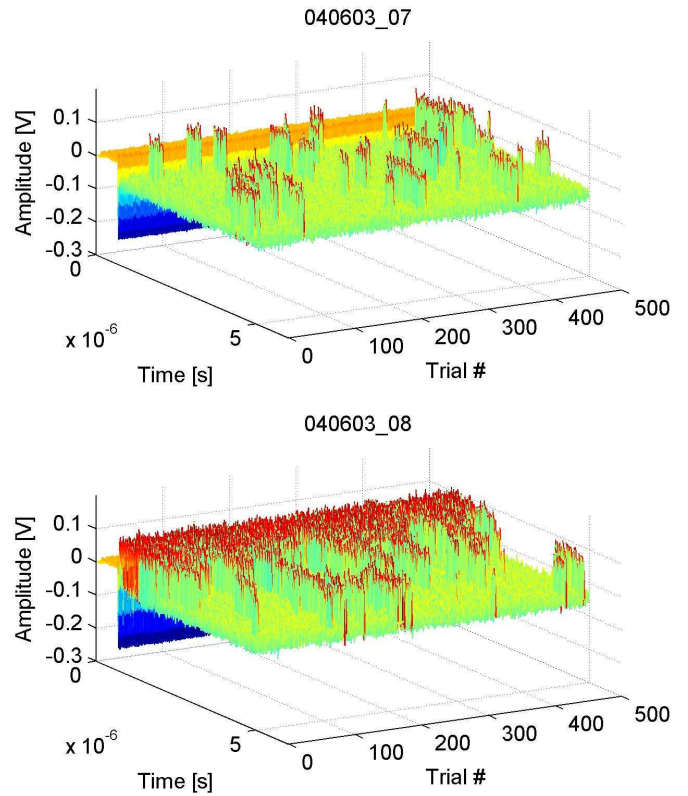


Fig. 8. RTS is seen to decay back to 'low' state briefly after turn-on (lower figure). Steady state behaviour of same device (upper figure).

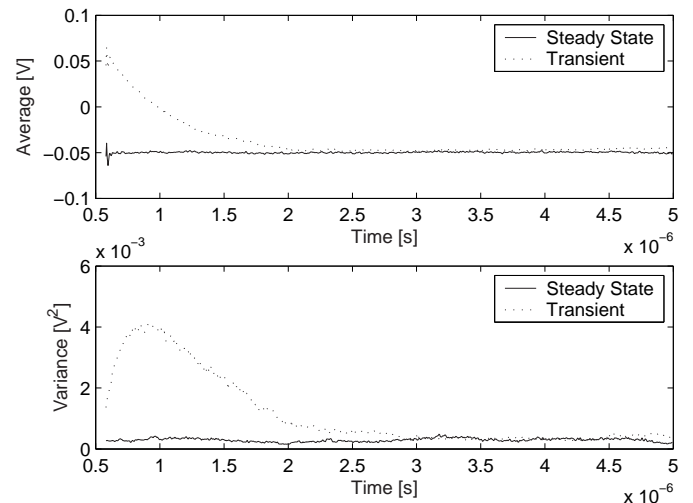


Fig. 9. Average and variance of noise voltage for the device of fig. 8.

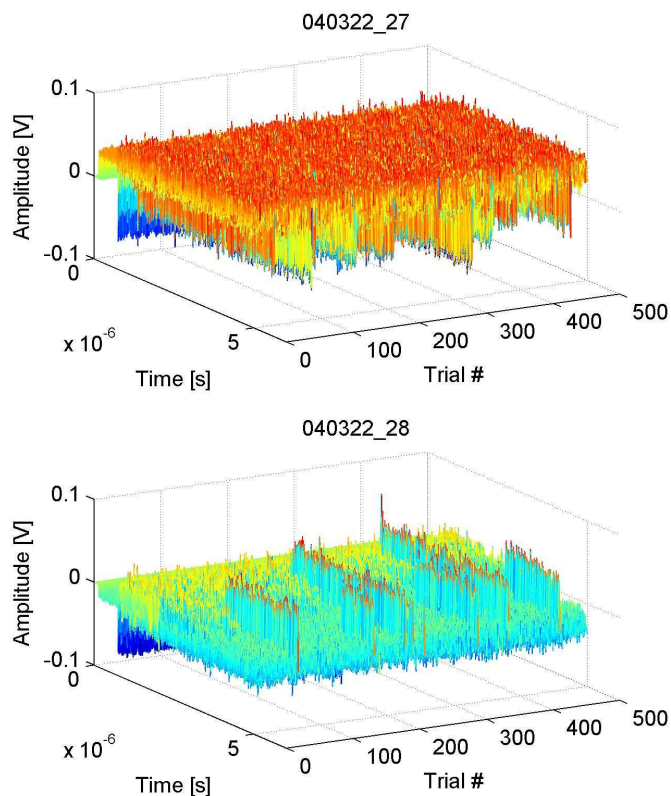


Fig. 10. RTS is mostly in the 'high' state in the steady state (upper figure), while immediately after turn-on, it is mostly in the 'low' state (lower figure).

sort of traps will be encountered in particular MOSFET, we are unable to predict the sort of behaviour that will be exhibited by a device in steady state, let alone transient conditions.

## VI. CONCLUSION

In this paper, we have presented visualisation techniques for Random Telegraph Signals in MOSFETs. We have given simple and very insightful ways to examine the time-domain transient behaviour of these single-electron effects. Though we have not done so in the present work, it is possible to extend the method to assign a physical 'trapped' and 'detrapped' state to the discrete amplitude levels observed in our experiments. Another obvious extension of the method is to observe the same device on different time scales. We have here used  $5\mu\text{s}$  after each turn-on transient (the 'fast' time axis), and performed approximately 1 measurement per second (the 'slow' time axis). Examining an RTS on even more time scales is easy and possible. Finally, statistical work needs to be done to better describe the probability of encountering a particular type of trap in a device. Only after measurement of

significant numbers of devices are we able to state with any degree of certainty what sort of behaviour the designer may expect from the MOSFET under steady state and under transient conditions, leading to more optimal analog CMOS designs.

## REFERENCES

- [1] E. A. M. Klumperink, S. L. J. Gierkink, A. P. van der Wel, and B. Nauta, "Reducing MOSFET  $1/f$  Noise and Power Consumption by Switched Biasing", *IEEE Journal of Solid-State Circuits*, Vol. 35, No. 7, July 2000, pp. 994-1001.
- [2] M. S. Keshner, "1/f Noise", *Proceedings of the IEEE*, Vol. 70, No.3, March 1982, pp. 212-218.
- [3] D. R. Wolters and A. T. A. Zegers- van Duijnhoven, "Modeling  $1/f$  noise of electronic devices", *Proceedings of the 14<sup>th</sup> International Conference on Noise in Physical Systems and 1/f Fluctuations (ICNF)*, July 1997, pp. 471-477.
- [4] P. H. Handel, "New insights on fundamental  $1/f$  noise theory and applications", *Proceedings of the 16<sup>th</sup> International Conference on Noise in Physical Systems and 1/f Fluctuations (ICNF)*, October 2001, pp. 584-589.
- [5] F. N. Hooge, "1/f noise is no surface effect", *Physica*, Vol. 29A, No. 3, April 1969, pp. 139-140.
- [6] T. G. M. Kleinpenning, "On  $1/f$  Noise and Random Telegraph Noise in very small Electronic Devices", *Physica B*, No. 164, 1990, pp 331-334.
- [7] M. J. Kirton and M. J. Uren, "Noise in solid-state microstructures: A new perspective on individual defects, interface states and low-frequency ( $1/f$ ) noise", *Adv. Phys.*, Vol. 38, no. 4, 1989, pp. 367-468.
- [8] A. L. McWorther, "1/f noise and germanium surface properties", *Semiconductor Surface Physics*, University of Pennsylvania press, 1957, pp 207.
- [9] A. Nemirovsky and A. Ron, "A New approach to carrier trapping-detrapping  $1/f$  noise", *Proceedings of the 14<sup>th</sup> International Conference on Noise in Physical Systems and 1/f Fluctuations (ICNF)*, July 1997, pp. 85-88.
- [10] K. K. Hung, P. K. Ko, C. Hu and Y. C. Cheng, "A Unified Model for the Flicker Noise in Metal-Oxide-Semiconductor Field-Effect Transistors", *IEEE Trans. Electron Devices*, Vol. 37, No. 3, March 1990, pp. 654-665.
- [11] K. S. Kundert, "Introduction to RF Simulation and Its Application", *IEEE Journal of Solid-State Circuits*, Vol. 34, No. 9, Sept. 1999, pp. 1298-1319.
- [12] I. Bloom and Y. Nemirovsky, "1/f noise reduction of metal oxide semiconductor transistors by cycling from inversion to accumulation," *Applied Physics Letters*, Vol. 58, No. 15, April 1991, pp. 1664-1666.
- [13] A. P. van der Wel, E. A. M. Klumperink, S. L. J. Gierkink, R. F. Wassenaar, and H. Wallinga, "MOSFET  $1/f$  noise measurement under switched bias conditions", *IEEE Electron Device Letters*, Vol. 21, No. 1, Jan. 2000, pp. 43-46.
- [14] S. Machlup, "Noise in Semiconductors: Spectrum of a Two-Parameter Random Signal", *Journal of Applied Physics*, Vol. 25, No. 3, March 1954, pp. 341-343.
- [15] A. P. van der Wel, E. A. M. Klumperink and B. Nauta, "Effect of switched biasing on  $1/f$  noise and random telegraph signals in deep-submicron MOSFETs", *Electronics Letters*, Vol. 37, No. 1, 4th Jan. 2001, pp. 55-56.
- [16] A. P. van der Wel, E. A. M. Klumperink, L. K. J. Vandamme and B. Nauta, "Modeling Random Telegraph Noise Under Switched

- Bias Conditions Using Cyclostationary RTS Noise”, *IEEE Transactions on Electron Devices*, Vol. 50, No. 5, May 2003, pp 1387-1384.
- [17] J. S. Kolhatkar, E. Hoekstra, C. Salm, A. P. van der Wel, E. A. M. Klumperink, J. Schmitz and H. Wallinga, ”Modeling of RTS Noise in MOSFETs under Steady-State and Large-Signal Excitation”, *IEDM 2004*, Accepted for publication.
- [18] E. Hoekstra, ”Random Telegraph Noise in MOSFETs- Time domain analysis under transient conditions”, *MSc. report, University of Twente*, August 2004, Report no. 068.109.